Tech Science Press

Melatonin ameliorates docetaxel-induced mitochondrial oxidative toxicity and cytokine generation in the laryngo-tracheal epithelial cell

Sinem Gökçe Kütük[1]; Mustafa Nazıroğlu[2,3,*]

[1] Department of Otorhinolaryngology, Aydın State Hospital, Aydın, 09100, Turkey
[2] Department of Biophysics, Faculty of Medicine, Suleyman Demirel University, Isparta, 32000, Turkey
[3] Drug Discovery Unit BSN Health, Analyses, Innovation, Consultancy, Organization Agriculture Ltd., Göller Bölgesi Teknokenti, Isparta, 32260, Turkey

Abstract: A protective action of melatonin (MELAT) on docetaxel (DCT)-induced inflammation, apoptosis, and reactive free oxygen radical (fROS) generation values via blocking of TRPM2 calcium-permeable channel was investigated in different cells except for laryngo-tracheal epithelial (LT-Epi) cells. Hence, the protective action of MELAT on DCT-induced oxidative toxicity and inflammation in LT-Epi tissue and cells of mice were investigated in the current study. MELAT treatment ameliorated DCT-induced mitochondrial ROS in the LT-Epi cells by reducing the generation of fROS (cytosolic and mitochondrial), lipid peroxidation, and depolarization of the mitochondrial membrane, while increasing reduced glutathione (GSH), GSH peroxidase, and total antioxidant status. In addition, DCT-induced increases of cytokine (IL-1β, IL-6, and TNF-α) generations were also diminished in the LT-Epi tissue by MELAT treatment. Furthermore, MELAT treatment increased viability and count of the cells followed by decreasing levels of cell death, caspase -3, and -9. The TRPM2 activity was also reduced by MELAT and TRPM2 channel blocker (ACA) treatments. In conclusion, MELAT modulated the increase of DCT-induced LT-Epi cell death by inhibiting mitochondrial oxidative stress and TRPM2 channel activity. Hence, DCT-caused side cell death, oxidant, and inflammatory actions in the LT-Epi were diminished via the treatment of MELAT.

Abbreviations

ACA: N-(p-amylcinnamoyl) anthranilic acid
DCF: 2',7'-dichlorofluorescein
DCFH-DA: 2',7'-dichlorodihydrofluorescin diacetate
DCT: docetaxel
DMEM: Dulbecco's Modified Eagle's Medium
ELISA: enzyme-linked immunosorbent assay
GSH: reduced glutathione
GSH/Px: glutathione peroxidase
H₂O₂: hydrogen peroxide
IL: interleukin
IL-1β: interleukin 1beta
LPx: lipid peroxidation
LT-EPi: laryngo-tracheal epithelial
MiMP: mitochondrial membrane potential
PI: propidium iodide
fROS: reactive free oxygen species

TAS: total antioxidant status
TNF-α: tumor necrosis factor alpha
TRPM2: transient receptor melastatin 2

Introduction

Docetaxel (DCT) treatment in cancer patients induces long-term survival as compared to a surgical application (Ishikawa *et al.,* 2015). Hence, DCT is a chemotherapeutic agent with an effective spectrum in human for treating several cancer cells, including cells of head, larynx, and neck cancers (Chan *et al.,* 2015; Starobova and Vetter, 2017). Recent reports indicate that DCT has major adverse side effects, including nephrotoxicity (Mohri *et al.,* 2018), testis toxicity (Sarıözkan *et al.,* 2017; Baş and Nazıroğlu, 2019a), brain injury (Ataizi *et al.,* 2019), and neck region cancers of patients (Haxel *et al.,* 2016). Within possible molecular pathways in the DCT-induced tissue adverse effect in the larynx, generations of excessive reactive free oxygen radical (fROS), inflammation, and apoptosis have been reported (Yanar *et al.,* 2016). DCT-induced fROS generations are an unbalanced redox reaction in the brain (Tabaczar *et al.,* 2017;

Ataizi *et al.*, 2019), testis (Sarıözkan *et al.*, 2017; Baş and Nazıroğlu, 2019a), and kidney (Baş and Nazıroğlu, 2019b), resulting decrease in the productions of lipid and DNA oxidations as lipid peroxidation. However, excessive fROS production may also lead to oxidative stress in the laryngo-tracheal epithelial (LT-Epi) cells during the DCT treatment and it has not been clarified yet.

In addition to the excessive fROS generation, cytokine generations such as IL-6 and IL-1β are responsible for the progression of tumors (Niu *et al.*, 2014; Bossi *et al.*, 2016; Shi *et al.*, 2018; Hoshikawa *et al.*, 2018). As a member of cytokines, tumor necrosis factor-alpha (TNF-α) is a key marker in the laryngo-tracheal physiological process and invasion of head and neck cancers (Bossi *et al.*, 2016; Hoshikawa *et al.*, 2018). TNF-α generation was increased during the tumor progression and treatment with chemotherapeutic agents, including DCT (Bossi *et al.*, 2016; Hoshikawa *et al.*, 2018). Cell death and cytokine generation are induced by excessive generation of fROS (Childs *et al.*, 2014; Ataizi *et al.*, 2019). Hence, inhibition of the DCT-induced fROS generation by antioxidant markedly decreases the cytokine generations (Rodriguez-Garcia *et al.*, 2013). DCT administration caused up-regulation of apoptosis, TNF-α, and IL-6 levels were diminished in mice by selenium treatment (Wang *et al.*, 2015; Gökçe and Nazıroğlu, 2020). These reports highlight the critical action of antioxidant treatment on DCT-induced TNF-α, IL-1β, and IL-6 generation in normal cells. Furthermore, chemotherapeutic agents increase the level of fROS through the induction of mitochondrial dysfunction (Nazıroğlu and Braidy, 2017). Accumulating evidence indicates that treatment with chemotherapeutic agents, including DCT, induces excessive generation of fROS and apoptosis via the release of caspase -3 and -9 in several cells except for LT-Epi cells (Hung *et al.*, 2015; Sakallı Çetin *et al.*, 2017; Lanza-Jacoby and Cheng, 2018). Hence, the subject should be investigated in the LT-Epi cells.

Melatonin (MELAT) is briefly synthesized in the pineal gland of humans and vertebrates from tryptophan. However, it is also produced in other cells of the body (Reiter *et al.*, 2013). MELAT modulates several physiological and biological functions of body cells because it is a multitasking hormone (Reiter *et al.*, 2013). MELAT acts a strong antioxidant role against the chemotherapy-induced fROS generation in different tissues via an increase of antioxidant enzymes (Ekmekcioglu, 2014; Carrasco *et al.*, 2015). Results of a recent study reported that MELAT treatment protected larynx mucosa from environmental tobacco smoke-induced excessive fROS generation and lipid peroxidation via the increase of antioxidant enzymes (Donmez *et al.*, 2016). The protective action of MELAT against cisplatin-induced tissue injury in the larynx of rats was also recently reported. Transient receptor potential (TRP) melastatin 2 (TRPM2) is a cation channel, and it is also permeable to calcium ion (Ca^{2+}) in the cell membrane. The main activators of TRPM2 are ADP-ribose (ADPR) and oxidative stress (Nazıroğlu and Lückhoff, 2008). Protective roles of MELAT against oxidative injury and apoptosis via blocking TRPM2 activity in the brain of rodents were reported (Carrasco *et al.*, 2018; Ataizi *et al.*, 2019). Contrary to the reports, MELAT also plays pro-oxidant and pro-apoptotic roles in leukocytes of patients with cancer (Bejarano *et al.*, 2011). Low MELAT receptor levels were reported in patients with cancer (Nemeth *et al.*, 2011). Recently, protective actions of MELAT on chemotherapy-induced oxidative toxicity and inflammation markers (TNF-α, IL-1β, and IL-6) were also reported (Nemeth *et al.*, 2011; Childs *et al.*, 2014; Nopparat *et al.*, 2017).

In the present research, we investigated the modulator action of MELAT on DCT-caused cell death, mitochondrial oxidative toxicity, and inflammation in the mice LT-Epi cells.

Materials and Methods

Animals and isolation of laryngo-tracheal epithelium (LT-Epi)
The study was approved by a local ethical committee (Burdur Mehmet Akif University (BMAU), Burdur, Turkey) (Protocol Number: 2019-482). Thirty-two C57BL/6j mice (male; 20 g and 6–8 weeks) were purchased from BMAU. The LT-Epi tissue and cells were isolated, as described previously (Zhou *et al.*, 2017). Summarily, the animals were euthanized under anesthesia, and LT-Epi tissue excised under sterile conditions and then cultured in a medium containing 45% Ham's F-12, 45% DMEM, 10% fetal bovine serum, and 1% antibiotic combination. The LT-EPi cells were then obtained from the LT-Epi tissues for analysis.

Experimental groups
The 32 animals were divided into equal four groups as control, MELAT, DCT, and their combination (DCT+MELAT). Placebo and MELAT administration to the mice were intraperitoneally performed for 7 days. A single dose of DCT was also intraperitoneally given to the animals (Tab. 1). Animals in the control group received a placebo (0.9% w/v). Animal in the second (MELAT) group received MELAT (10 mg/kg/day) for 7 days (total of seven doses) (Ataizi *et al.*, 2019). Animals in the third (DCT) group

TABLE 1

Details of treatments in the control and experimental groups

Doses	Control	MELAT	DCT	DCT+MELAT
Placebo (0.9% w/v) for 7 days	+	–	+	–
MELAT (10 mg/kg/day) for 7 days	–	+	–	+
DCT (30 mg/kg and single dose)	–	–	+	+

received DCT (30 mg/kg) (Kim et al., 2017; Ataizi et al., 2019). Animals in the last group (DCT+MELAT) group received a combination of DCT and MELAT. All injections were performed between 08.00 and 09.00 a.m.

After dissolving MELAT in DMSO, it was diluted in the sterile physiological saline (0.9% w/v) as described previously (Kahya and Nazıroğlu, 2016). At the end of the last MELAT injection, LT-Epi tissues of all mice were taken under anesthesia, and cells were obtained from the tissue as described above. Half of the tissue was stored at −33°C for the antioxidant, lipid peroxidation (LPx), and cytokine assays, although remaining samples were used for obtaining LT-Epi cells for using apoptosis, cell viability, cell death, cell count, membrane depolarization of mitochondria (MiMP), fROS, caspase -3 and -9 analyses.

Lipid peroxidation (LPx) measurement in the LT-Epi tissue samples
LPx concentrations in the samples were measured according to a spectrophotometric method (Botsoglou et al., 1994). After homogenization of the tissue samples in a tube by an ultrasonic homogenizer, the supernatant of tissue samples was mixed with 1 mL of 20% trichloroacetic acid and 0.5% thiobarbituric acid mixture. After boiling and cooling procedures of the mixture, the supernatant was obtained by centrifugation at $1500 \times g$, and then the supernatant was transferred to a new clean tube. The absorbance pink color in the supernatant of LT-Epi tissue samples was detected at 532 nm by using a spectrophotometer (*Cary 60* UV-Vis). Different concentrations of MDA were used as standards. The LPx concentrations were expressed as μmol/g protein.

Determinations of total antioxidant status (TAS), total tissue protein, reduced glutathione (GSH), and glutathione peroxidase (GSH/Px)
The four analyses were performed by using the spectrophotometer (*Cary 60* UV-Vis) as described previously (Kahya and Nazıroğlu, 2016). TAS concentration in the tissue samples was detected via a commercial kit of Mega Tip Inc. (Gaziantep, Turkey) (Erel, 2004). Total tissue protein content in the tissue samples was measured via the method of Lowry, as described previously (Kahya and Nazıroğlu, 2016).

The GSH concentration in the LT-Epi tissues was analyzed at 412 nm via enzymatic conjugation of glutathione to 1-chloro-2,4-dinitrobenzene (Saxena et al., 1992).

GSH/Px activity of the LT-Epi tissue samples was analyzed at 412 nm (Lawrence and Burk, 1976).

Cell viability and cell count analyses in the LT-Epi cells
Cell viability analyses in the cells were performed in an Infinite pro200 model microplate reader (Tecan Austria GmbH, Groedig, Austria) by reduction of tetrazolium salts of the MTT (Sakallı Çetin et al., 2017; Gökçe and Nazıroğlu, 2020). After calculation of the date as optic density per mg protein, the %-increase of control (experimental/control) value was used for expression of MTT values. The MTT analyses were performed in the eight samples (N = 8).

A Casy Modell TT automatic cell counter (Roche, Germany) was used for assaying the cell counts of LT-Epi cells. The mean values of cell numbers were indicated as $\times 10^6$ cells/mL.

Apoptosis and caspase assays in the LT-Epi cells
Apoptosis measurement was performed according to a commercial APOPercentage dye of Biocolor Ltd. (Northern Ireland) (transfer of phosphatidylserine to an extracellular side of the cell membrane allows the transport of the dye into the cytosol of the cell) by using Infinite pro200 microplate reader as described in our study (Sakallı Çetin et al., 2017). The %-increase of control was also used for expressing apoptosis values.

The assays of caspase -3 and -9 activities with caspase medium were based on methods previously reported (Gilbert et al., 2016; Sakallı Çetin et al., 2017; Gökçe and Nazıroğlu, 2020). Mainly, the assays were based on cleavages of caspase -3 (Ac-DEVD-AMC) and -9 (Ac-LEHD-AMC) substrates in the cells. Accumulations of AMCs were in the Infinite pro200 (Ex; 365 nm; Em: 460 nm). The mean values were presented as a %-increase of control.

Analyses of intracellular fROS generation and MiMP level in the LT-Epi cells
Intracellular fROS and MiMP levels were captured in the Infinite pro200 by using 2',7'-dichloro-dihydro fluorescein diacetate (DCFH-DA) and JC-1 stains, respectively as described in a previous study (Joshi and Bakowska, 2011). In brief, the DCFH-DA (5 mM) and JC-1 (10 mM) stains were added to the cell culture flask. After 30 min, the medium was removed from the cells by washing twice with 1× PBS. Then, the cells were re-suspended in the 400 mL 1× PBS within the 96-black plates. The analyses were performed in the plate reader. The mean values of DCFH-DA and JC-1 were expressed as %-increase of the control.

Cytokine measurements in the LT-Epi tissue
For mouse cytokine measurements in the supernatant of LT-Epi tissue, the IL-1β, IL-6, and TNF-α levels were assayed according to the protocol provided with the enzyme-linked immunosorbent assay kit (R&D Systems, Istanbul, Turkey) at 450 nm as described in our study (Ataizi et al., 2019). The mean data of IL-1β, IL-6, and TNF-α levels were indicated as ng/mg protein.

Determination of live (Hoechst) and death (propidium iodide, PI) ratio in the LT-Epi cells
Images of live and dead cells in the four groups were captured in a laser confocal microscope (LSM 800, Zeiss, Ankara, Turkey) with a 20× objective. After incubation of the LT-Epi cells with PI (5 μg/mL) and Hoechst 33342 (1 μM) fluorescent stains for 30 min, the cells were washed and re-suspended in the 400 mL 1× PBS as described in previous studies (Li and Jiang, 2018; Gökçe and Nazıroğlu, 2020). PI (red) and Hoechst (blue) images were captured in the confocal microscope by using ZEN program. Changes in the PI/Hoechst ratios were expressed as %.

Bright field (BF) and the cell counts in the LT-Epi cells
The BF imaging and cell count in the cells were determined in a CCD Zeiss camera with high-performance (Axiocam 702 mono). Details of the analyses were given in our study (Gökçe and Nazıroğlu, 2020).

Electrophysiology

Patch-clamp analyses (whole-cell) of the LT-Epi cells were performed at room temperature by using the EPC10 patch-clamp set (HEKA, Lamprecht, Germany). Holding potential in the voltage-clamp analyses was kept as −60 mV. We used the same patch and chamber buffers in our experiments (Sakallı Çetin *et al.*, 2017; Ataizi *et al.*, 2019). For chelating Ca^{2+}, we used Na^+ free extracellular buffer $NMDG^+$ (*N*-methyl-D-glucamine) instead of Na^+ (150 mM and pH = 7.2). The results were expressed as current density as (current amplitudes/cell capacitance, pA/pF). Well-known TRPM2 activators and inhibitors are hydrogen peroxide (H_2O_2) and N-(p-amylcinnamoyl) anthranilic acid (ACA), respectively (Hara *et al.*, 2002; Kraft *et al.*, 2006; Nazıroğlu and Lückhoff, 2008). Hence, extracellular H_2O_2 (10 mM) and ACA (25 μM) were used for activation and inhibition of TRPM2, respectively (Nazıroğlu and Lückhoff, 2008; Ataizi *et al.*, 2019).

Statistical analysis

For expression of the results, mean ± standard deviation (SD) was used. A Least Significant Difference (LSD) test and Mann–Whitney's analyses of Statistical Package for the Social Sciences (SPSS) program were used for detecting significance level and *P*-values.

Results

MELAT decreased DCT-caused apoptosis levels, but increased cell viability

In previous studies (Ataizi *et al.*, 2019; Gökçe and Nazıroğlu, 2020), responses of apoptosis to the treatments of chemotherapeutic drugs in tumor cells were assayed by using the cell viability test and commercial apoptosis kits. These tests are now widely accepted as two valid ways to examine cell proliferation. To evaluate the effects of DCT and MELAT on LT-Epi cells, we used the MTT assay and commercial kit for assaying the cell viability and apoptosis, respectively.

As was indicated in Fig. 1a, DCT injection caused an increase of apoptosis levels, and the levels of apoptosis were higher in the DCT group compared with the groups of Ctr and MELAT (*P* < 0.05). However, the treatment of MELAT in the DCT+MELAT group diminished the apoptosis level,

and its level was lower in DCT+MELAT group as compared with the groups of DCT only (*P* < 0.05). As indicated in Fig. 1b, DCT injection downregulated the levels of MTT, although the MELAT treatment upregulated the levels of MTT in the DCT+MELAT group (*P* < 0.05). Importantly, we observed that MELAT injection to the mice decreased the apoptosis, but it increased the viability of the LT-Epi cells.

MELAT treatment decreased DCT-induced upregulation of caspase activity, JC-1, fROS, and antioxidant levels in the LT-Epi cells

During several cellular metabolisms, inactive pro-caspases are constitutively synthesized in body cells (Reiter *et al.*, 2013). It was reported that molecular pathways of apoptosis in tumors, including laryngeal squamous cell carcinoma, contain an activation of caspases, including caspase -3 and -9 (Chrysovergis *et al.*, 2019).

In the present data, the DCT treatment caused an increase of caspase -3 (Fig. 2a) and -9 (Fig. 2b) activities, and their activities were higher in the groups of DCT compared with the groups of Ctr and MELAT (*P* < 0.001). However, the increase of caspase -3 and -9 was reduced in the DCT+MELAT by the MELAT injection (*P* < 0.001).

Mitochondria are the main sources of excessive fROS generation (Carrasco *et al.*, 2015). The generated fROS are inhibited in the mitochondria by antioxidants, including GSH and GSH/Px (Nazıroğlu, 2009). Apoptosis, as programmed cell death, is an electron transport system of molecular pathways involving pro-caspase actions, leading to the death of a cell (Chrysovergis *et al.*, 2019). During the electron transport system of molecular pathways, different key activations occur in the mitochondria, including the conventions of the pro-caspase -3 and -9 to active caspase -3 and -9 and excessive stimulation of fROS generations (Gökçe and Nazıroğlu, 2020). The electron transport system of mitochondria also induces loss of MiMP via excessive Ca^{2+} transport from the cytosol into mitochondria (Carrasco *et al.*, 2015). Hence, measurement of MiMP was used as an important parameter of mitochondrial function in the normal and tumor cells (Carrasco *et al.*, 2015).

The DCT treatment increased MiMP (Fig. 2c) and intracellular fROS production (Fig. 2d), and LPx level (Fig. 3a) (*P* < 0.001). However, the increase of fROS, MiMP,
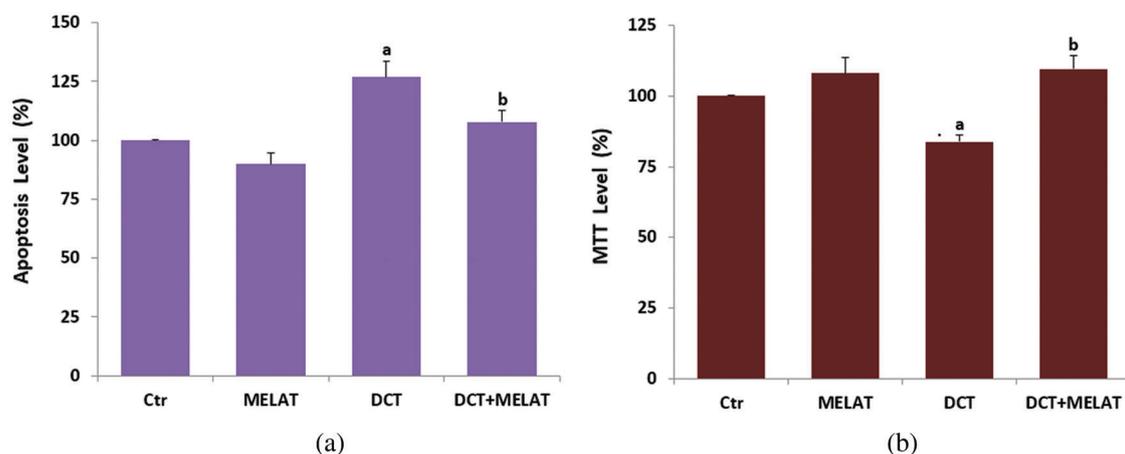
FIGURE 1. The MELAT injection diminished docetaxel (DCT)-induced apoptosis (a) and MTT (b) levels in the LT-Epi mice cells. (mean ± SD and N = 8; [a]*P* ≤ 0.05 compared with groups of untreated (control, Ctr) and MELAT. [b]*P* < 0.05 compared with DCT group).
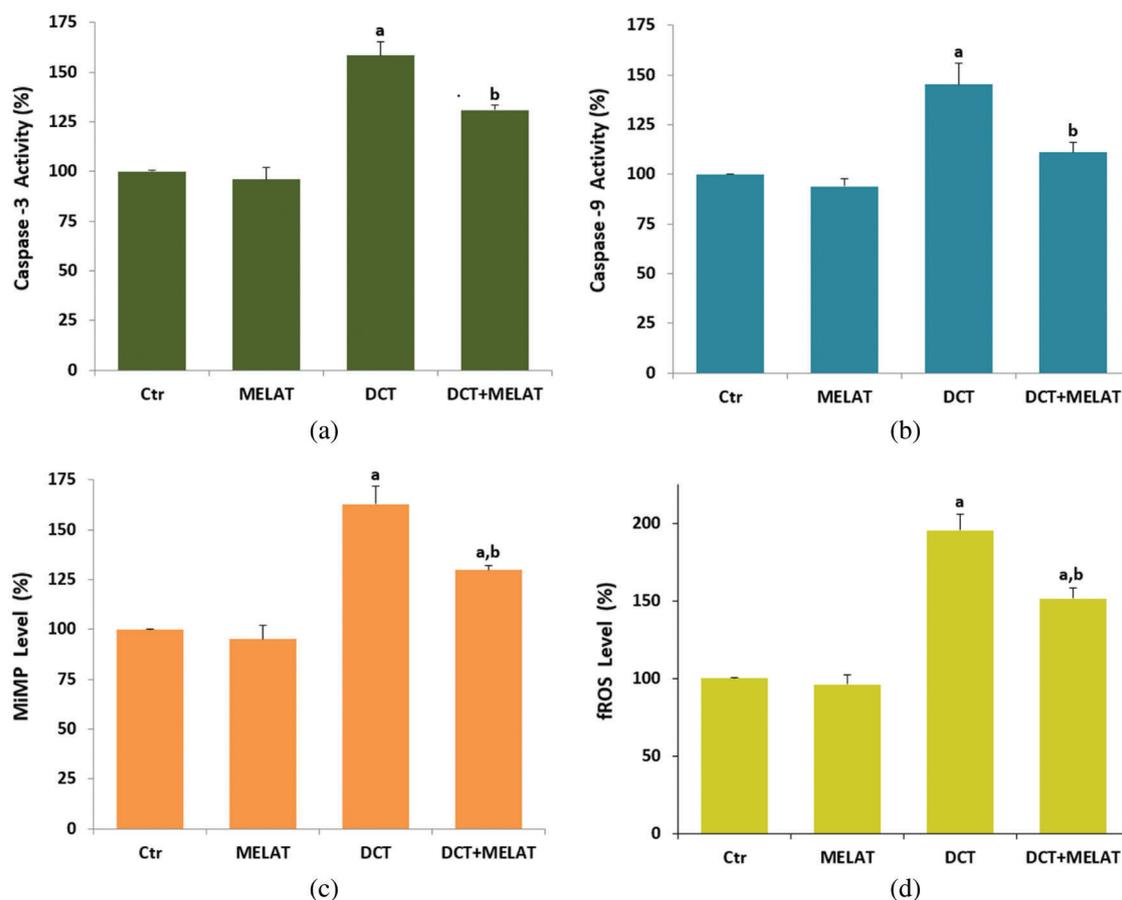
FIGURE 2. The effects of melatonin (MELAT) on docetaxel (DCT)-induced activations of caspase-3 (a), caspase -9 (b), the levels of MiMP (c) and fROS generation (d) in the LT-Epi cells of mice. (Mean ± SD and N = 8; [a]$P < 0.001$ and compared with control (Ctr) and MELAT groups. [b]$P < 0.001$ and compared with DCT group).

and LPx, were markedly decreased by the MELAT treatment ($P < 0.001$). DCT-induced deficiency of thiol group antioxidants was reported in experimental animals (Hung et al., 2015; Sarıözkan et al., 2017; Lanza-Jacoby and Cheng, 2018). In the current study, we investigated the values of TAS (Fig. 3b) and GSH (Fig. 3c), and GSH/Px (Fig. 3d) in the tissue samples. DCT caused a decrease in the TAS, GSH, and GSH/Px values compared with the groups of control and MELAT ($P < 0.001$). More interestingly, compared with the group of DCT, MELAT treatment stimulated the TAS, GSH levels, and GSH/Px activities in the tissue ($P < 0.001$).

DCT-induced LT-Epi cell death was reduced by the MELAT treatment
The laser confocal microscopy technique is one of the best techniques to image cell death. In the technique, Hoechst stain with blue color indicates live cells, whereas PI stain with red color indicates dead cells (Gomes et al., 2018). For detection of the dead/live cell ratio, the stains were used in several cells, including LT-Epi (Gökçe and Nazıroğlu, 2020). In the present study, the ratio of dead/live cells (Figs. 4a, 4c, and 4d) in the LT-Epi cells of the DCT group was high compared with the groups of control and MELAT ($P < 0.001$). However, their ratios were diminished in the DCT +MELAT group by the MELAT treatment. In the current study, we imaged BF images of cell count in the four groups

(Figs. 4b and 4e). Structures of the cells in the BF records were degenerated by the DCT treatment, although they were recovered by the MELAT treatment. The number of LT-Epi cells was also lower in the groups of DCT compared with groups of control and MELAT, whereas its number was high in the group of DCT+MELAT group (Fig. 4e). In addition to the caspase and apoptosis results, the results of the ratios of dead/live cells further supported the protective action of MELAT on the cell death action of DCT in the LT-Epi cells.

MELAT decreased inflammation response after DCT treatment
As was indicated in Figs. 5a and 5b, DCT resulted in the upregulation of IL-1β and IL-6 generations in the cells, while the administration of MELAT was reduced these inflammatory cytokine generation levels ($P < 0.001$). In addition, we measured the levels of TNF- α in the culture medium, and its level was increased in the group of DCT ($P < 0.001$) (Fig. 5c). Treatment with MELAT obviously diminished the generation of TNF-α in the cells ($P < 0.05$ or $P < 0.001$).

MELAT modulated DCT-induced TRPM2 current density in the LT-Epi cells
After the observation of an increase in the concentration of fROS and LPx in LT-Epi cells of the DCT group, we suspected increased activity of TRPM2, because it is activated by fROS generations. Hence, we want to clarify the
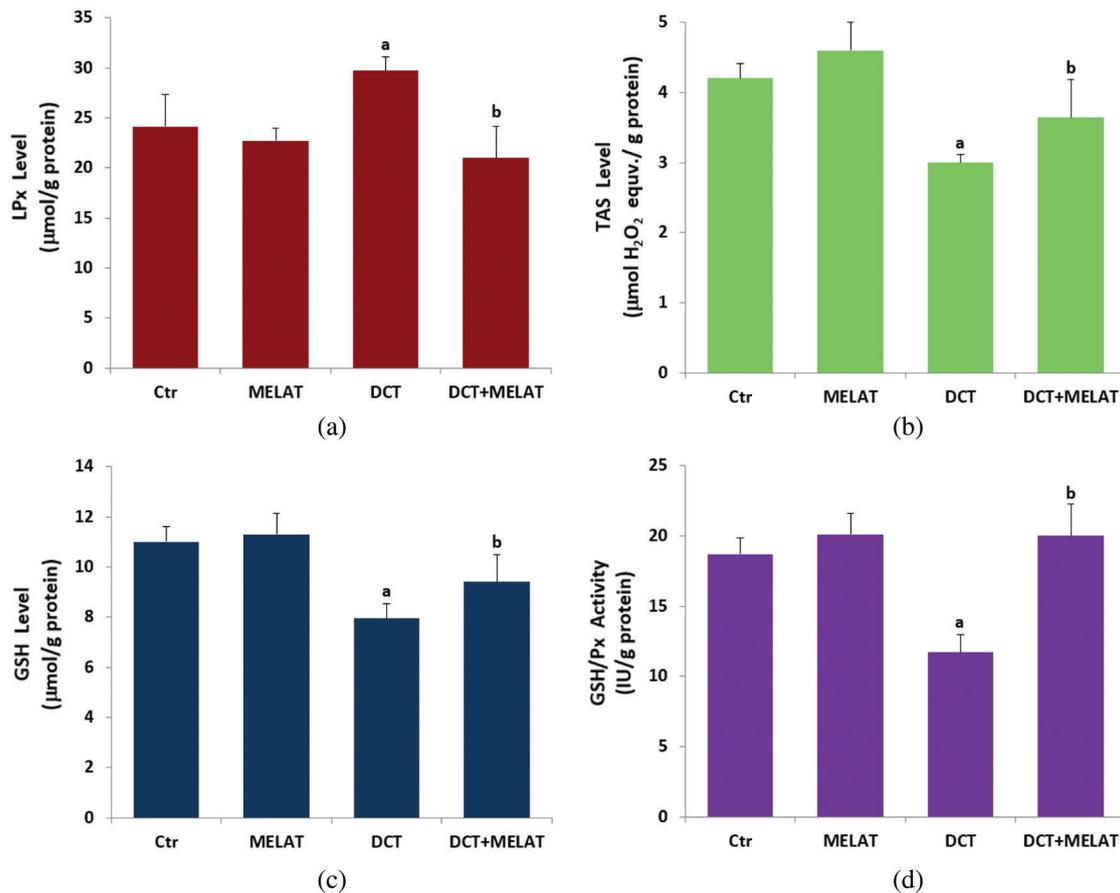
FIGURE 3. Melatonin (MELAT) decreased docetaxel (DCT)-induced lipid peroxidation (LPx) (a), but increased total antioxidant status (TAS) (b), reduced glutathione (GSH) level (c), and GSH peroxidase (GSH/Px) activity (d) in the LT-Epi tissue. (Mean ± SD and N = 8). The LPx, TAS, GSH, and GSH/Px analyses were spectrophotometrically (Cary 60 UV) performed in the tissue homogenate samples. ($^{a}P \leq$ 0.001 compared with the groups of untreated (Ctr) and MELAT. $^{b}P < 0.001$ compared with the group of DCT).

action of the TRPM2 on the Ca^{2+} entry in the cells by using the molecular electrophysiology analyses (whole-cell and voltage-clamp patch-clamp records). In the normal (untreated) cells, the H_2O_2-mediated TRPM2 activation was blocked by the TRPM2 blocker (ACA) and $NMDG^+$ (Fig. 6b). However, we observed the absence of TRPM2 activation in the control group (in the absence of the H_2O_2) (Fig. 6a). The pA/pF levels in the cells were higher in the control+H_2O_2 (123.80 pA/pF) group as compared with the control (6.35 pA/pF) (P < 0.001) (Figs. 6b and 6f); however, there was no TRPM2 activation through H_2O_2 stimulation in the cells of DCT in the pre-incubation of ACA (Figs. 6b and 6c). DCT-mediated upregulation of the TRPM2 pA/pF level was decreased in the cells by the MELAT injection, and its level was lower in the DCT+MELAT (7.21 pA/pF) (Fig. 6d) and MELAT (Fig. 6e) groups as compared to the group of DCT (337.57 pA/pF) (Figs. 6c and 6f) (P < 0.001). The electrophysiology results confirmed the involvement of TRPM2 on the DCT-mediated Ca^{2+} entry in the LT-Epi cells. The DCT-mediated TRPM2 pA/pF levels via downregulation of excessive fROS generation were diminished in the cells by the MELAT treatment.

Discussion

Accumulating evidence indicated that oxidative stress redox system is an important actor to promote chemotherapeutic

agent-mediated cytotoxicity, apoptosis, and TRPM2 activation via excessive generations of fROS within the cancer treatment molecular pathways (Kahya and Nazıroğlu, 2016; Sakallı Çetin et al., 2017; Zhou et al., 2017; Ataizi et al., 2019). Some tissues such as the brain and neurons have a high oxygen consumption rate. In addition, some tissues such as the lung and LT-Epi in the air pathways are mostly exposed to oxygen consumption. Hence, they are very sensitive to the adverse effects of fROS (Pariente et al., 2017). Due to the high oxygen consumption rate, LT-Epi tissue is sensitive to fROS-induced oxidative stress. Cells of the body are protected from the excessive generations of fROS by enzymatic antioxidants such as GSH/Px and superoxide dismutase and non-enzymatic antioxidants such as GSH and MELAT (Ekmekcioglu, 2014; Nopparat et al., 2017). Present literature data have displayed that DCT diminishes the antioxidant redox systems followed a significant decrease in the levels of GSH, TAS, and activities of GSH/Px and elevation in the generations of fROS and content of LPx (Yanar et al., 2016; Sarıözkan et al., 2017; Haxel et al., 2016; Ataizi et al., 2019; Baş and Nazıroğlu, 2019a; Baş and Nazıroğlu, 2019b; Gökçe and Nazıroğlu, 2020). H_2O_2 is converted to water in the cytosol of cells by the enzymatic effect of GSH/Px and TRPM2 channel activated by fROS (Hara et al., 2002; Nazıroğlu and Lückhoff, 2008; Nazıroğlu, 2009). In the current data, we
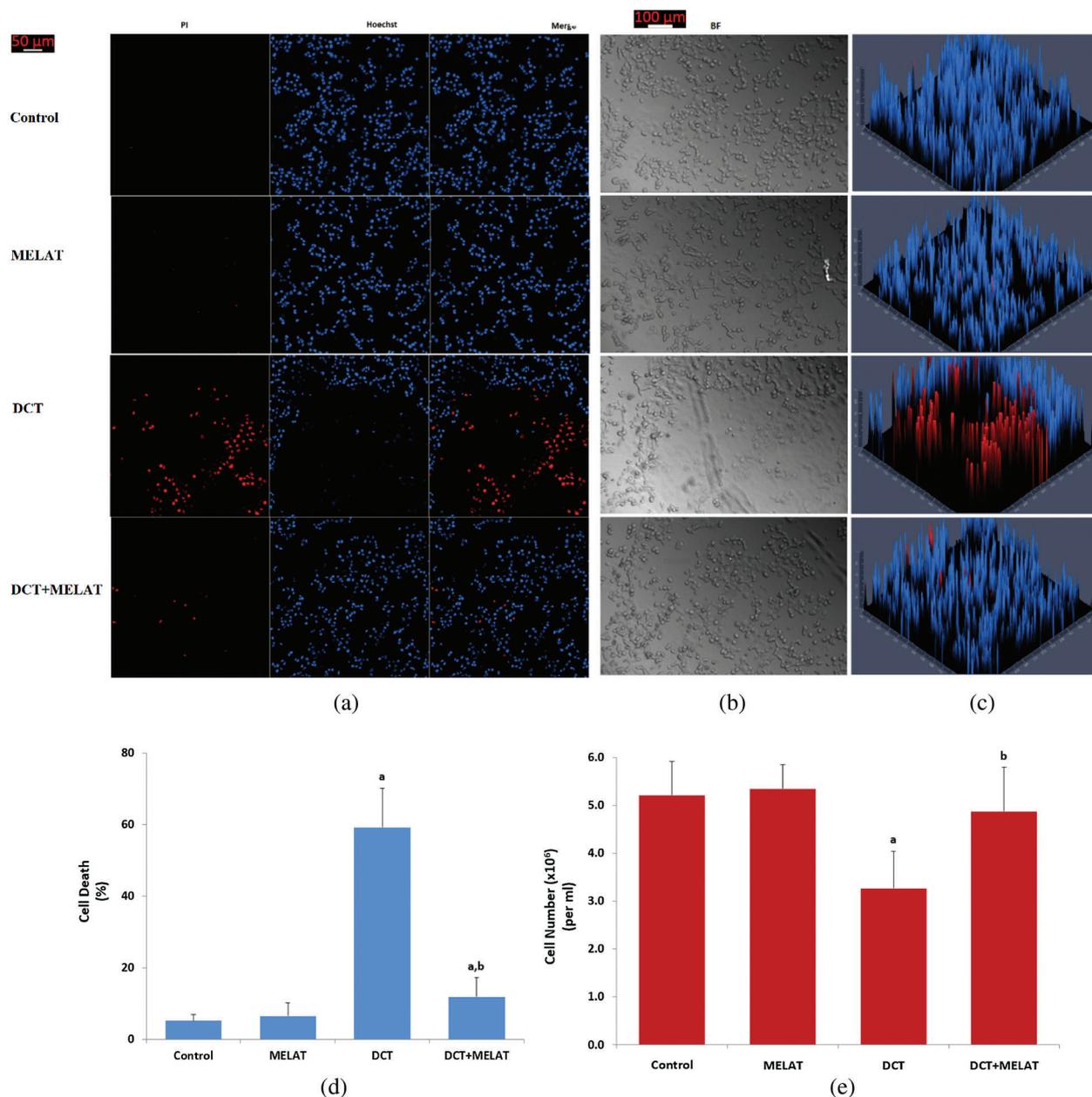
FIGURE 4. Melatonin modulated DCT-induced LT-Epi cell death and cell number changes. (Mean ± SD, N = 8. Scale bar: 50 μm).
(a) Representative image showing death (red: propidium iodide, PI) and live (blue: Hoechst 33342) staining of the cells. We also imaged bright field (BF) (b) and 2.5D (c) in the four groups by using the LSM800 laser confocal microscope. (d) The mean percentage of PI/Hoechst ratio. (e) Summary of the mean cell count in the four groups. ([a]$P < 0.001$ compared with the groups of untreated (Ctr) and MELAT. [b]$P < 0.001$ as compared with the group of DCT).

found for the first time that injection with MELAT inhibited the elevations of fROS and LPx through upregulation of GSH, GSH/Px, and TAS contents and down-regulation of TRPM2 channel activity in DCT-treated LT-Epi mucosa. Hence, the strong antioxidant action of MELAT decreased the DCT-mediated oxidative LT-Epi cytotoxicity.

We found negative synergic action between MELAT and DCT in the MiMP, apoptosis, caspase -3, and caspase -9 values in the LT-Epi cells, and their values were decreased by MELAT treatment. There is accumulating evidence that fROS-related programmed cell death (apoptosis) is one of the significant pathophysiological pathways of chemotherapeutic agent-caused normal tissue injury

(Bejarano *et al.*, 2011; Pariente *et al.*, 2017; Tabaczar *et al.*, 2017). If the chemotherapeutic agents such as cisplatin accumulate in the matrix of mitochondria, it results in a massive generation of fROS and dysfunction of mitochondrial, resulting in mitochondrial Ca^{2+} permeability and pro-apoptotic factor generations (Zhou *et al.*, 2017). It is well known that activation mitochondrial apoptotic proteins such as Bcl-2 activate caspases, including caspase-9 (Fig. 7). The modulator role of antioxidants, including MELAT on cisplatin-induced the caspase -3 and caspase-9 cascades in several tissues were reported (Hung *et al.*, 2015; Pariente *et al.*, 2017). In the present data, MELAT significantly reduced the cellular apoptosis confirmed by

(a)

(b)

(c)
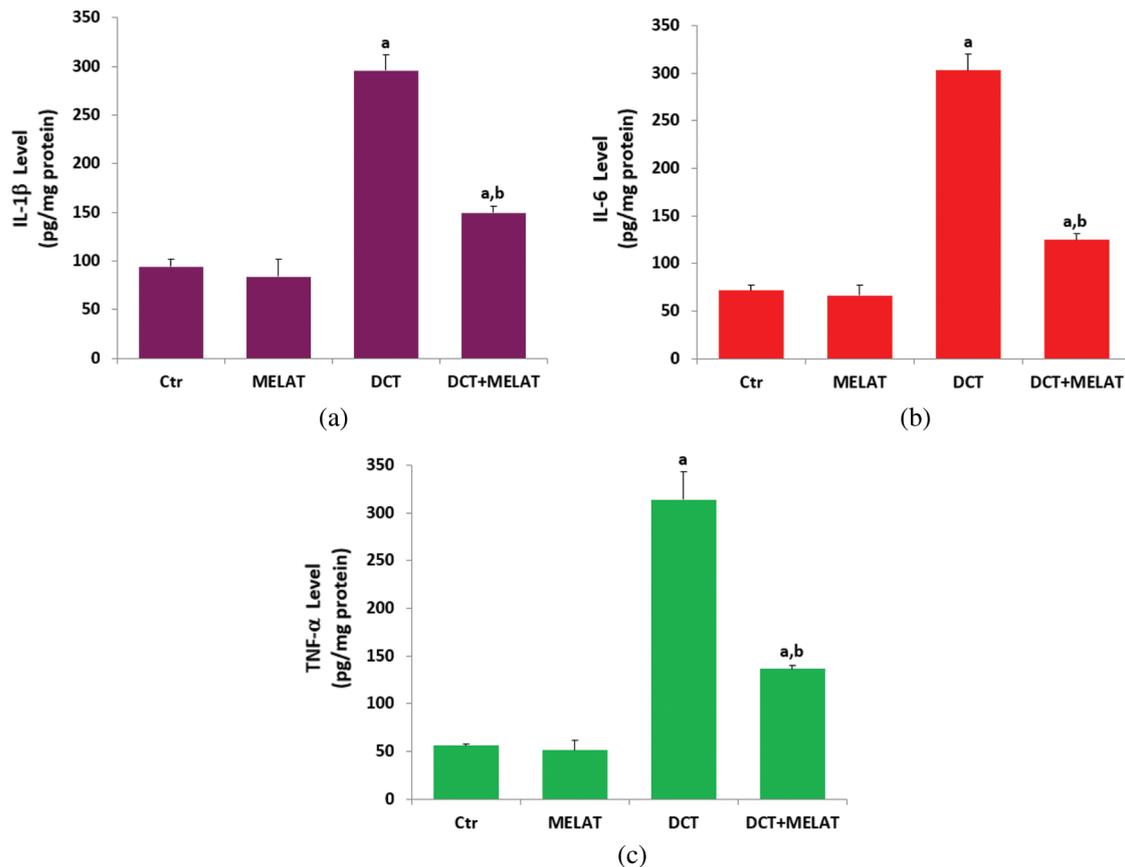
FIGURE 5. Melatonin (MELAT) reduced docetaxel (DCT)-induced cytokine generations in the mouse LT-Epi tissue homogenate. (Mean ± SD, N = 8).
The IL-1β (a), IL-6 (b), and TNF-α (c) levels in the tissue homogenate were assayed in ELISA via commercial kits. ([a]$P < 0.001$ compared with the groups of untreated (Ctr) and MELAT. [b]$P < 0.001$ compared with the group of DCT).

commercial apoptosis kits and plate reader caspase-3 and -9 analyses in comparison with the DCT group.

In addition to the involvement of DCT-apoptosis via excessive fROS generation in normal tissues, fROS has been shown to act a major role in the releases of inflammatory cytokines and TRPM2 channel activation (Ataizi et al., 2019). Several studies demonstrated the anti-inflammatory effects of MELAT in chemotherapeutic agents (DCT and cisplatin)-treated animals and humans (Hung et al., 2015; Ataizi et al., 2019). Hence, we aimed that MELAT might exert anti-inflammatory and TRPM2 blocker actions on DCT-mediated LT-Epi cell oxidative injury in mice. The current cytokine and TRPM2 data showed that treatment with MELAT markedly reduced the activation levels of TRPM2, TNF-α, IL-1β, and IL-6 levels compared with the DCT group. Similarly, the increase of DCT-induced cytokine and TNF-α productions were promoted in prostate cancer cells by MELAT treatment

(Rodriguez-Garcia et al., 2013). It was more recently indicated that DCT-mediated TRPM2 channel activity was decreased in the hippocampus of mice by the MELAT treatment (Ataizi et al., 2019). Decreases of TNF-α, IL-1β, and IL-6 levels were reported in the neuroblastoma cells (SH-SY5Y) exposed to oxidative stress (H_2O_2) by MELAT (Nopparat et al., 2017).

In summary, the oxidant, inflammatory, and apoptotic side actions of DCT in the LT-Epi cells of mice were inhibited by antioxidant MELAT. The essential mechanism in the MELAT action is caused by inhibition of mitochondrial fROS-related pro-apoptotic factors such as caspase -3, caspase -9, and excessive Ca^{2+} influx (via inhibition of TRPM2), but the increase of GSH/Px, GSH, and TAS values. Hence, MELAT may have a beneficial effect on the protection of DCT-induced side effects (apoptosis, inflammation, TRPM2 activation, and oxidative cytotoxicity) in the tissue.
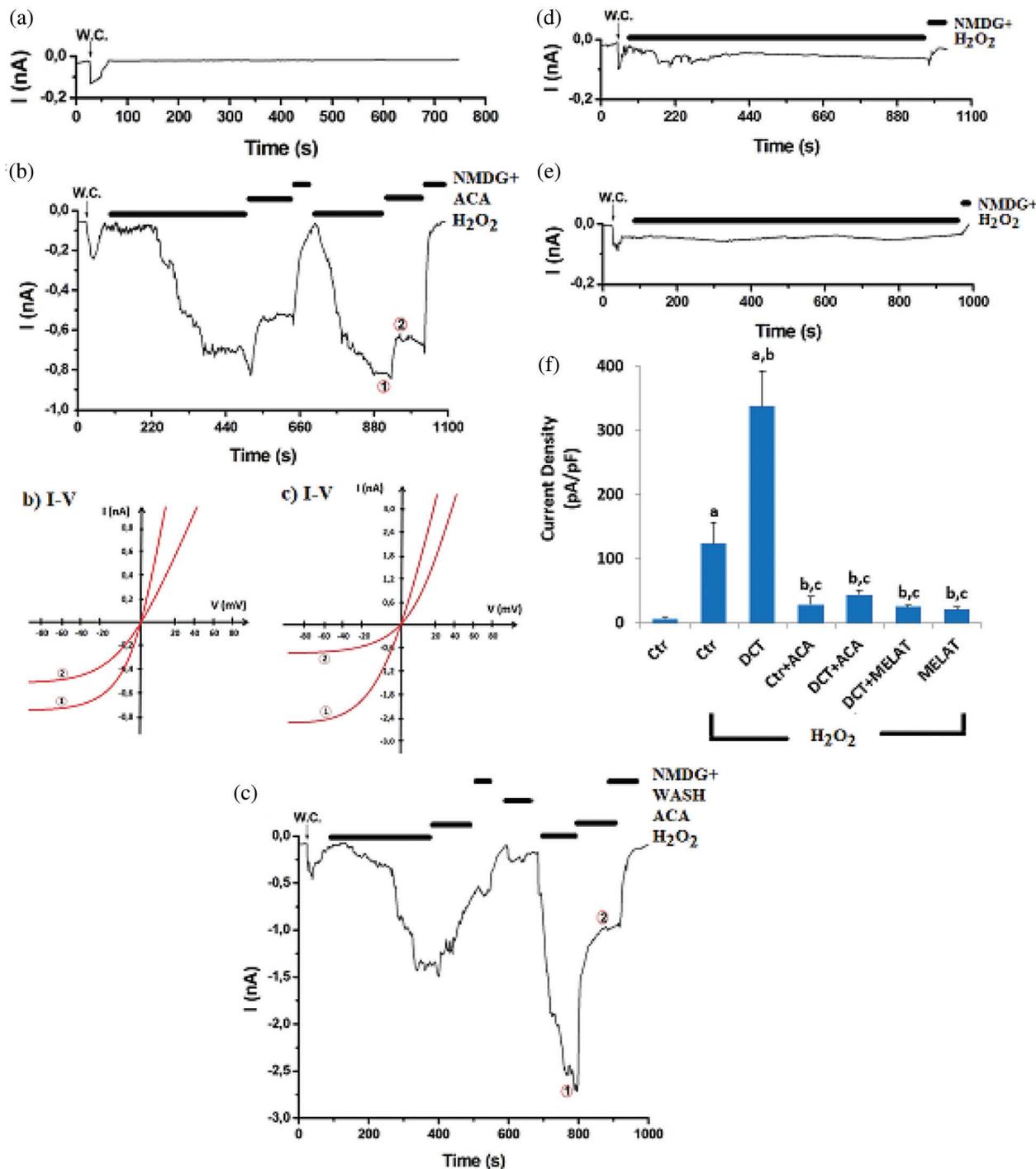
FIGURE 6. Melatonin (MELAT) treatment reduced docetaxel (DCT)-mediated upregulation of TRPM2 pA/pF levels in the TL-Epi cells. (mean ± SD; N = 8).

The TRPM2 pA/pF levels in the cells were gated by H_2O_2 (10 mM), whereas they were blocked by ACA (25 μM) and $NMDG^+$ (Na^+-free solution). W.C. is the abbreviation for "whole-cell". All cells (b-e except control group (a) were stimulated by H_2O_2 (a) Control (Ctr). (b) Ctr+ H_2O_2 group: Cells in the group were stimulated with H_2O_2 (c) DCT group: Cells of the DCT treated mice. (d) DCT+MELAT group: MELAT was injected into the mice after DCT treatment. Cells in the group were stimulated with H_2O_2. (e) MELAT group (without DCT treatment): Cells in the group were stimulated with H_2O_2. (f) TRPM2 channel current densities. The current unit of densities was indicated as pA/pF. ([a]$P < 0.001$ compared with untreated (Ctr) group. [b]$P < 0.001$ compared with Ctr+H_2O_2 group. [c]$P < 0.001$ compared with DCT+H_2O_2 group).
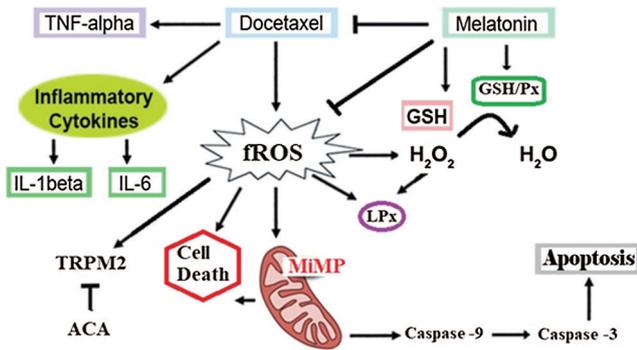
FIGURE 7. Summary of pathways involved in docetaxel (DCT)-induced cell death and free reactive oxygen radical (fROS) production via Ca^{2+} influx (TRPM2) inhibition by melatonin (MELAT). DCT is a chemotherapeutic agent, and its excessive fROS generation and apoptotic actions are inhibited in several cells by the antioxidant action of MELAT. The main mechanism in the anti-cell death effect of MELAT is caused by inhibition of fROS-mediated mitochondrial membrane potential (MiMP), caspase -3 and -9 activations. In addition, the protective action of MELAT on antioxidants [reduced glutathione (GSH) and glutathione peroxidase (GSH/Px)] in the LT-Epi cells initiates an antioxidant response that facilitates the neutralization of fROS and lipid peroxidation (LPx) into less harmful products. DCT increases the activation of cytokines and TRPM2 in the cells through excessive fROS generation, causing an increase of the TNF-α level. Hence, inhibition of the DCT-mediated fROS generation and Ca^{2+} influx by MELAT and TRPM2 blocker (ACA) decreased the TNF-α, IL-1β, and IL-6 productions.

Authors' Contributions: SGK formulated the present hypothesis and she was responsible for the plate reader and ELISA analyses. MN was responsible for writing the report and analyzing the patch-clamp, laser confocal microscope, and spectrophotometer analyses.

Availability of Data and Materials: The datasets analyzed during the current study are available from the corresponding author on reasonable request.

Conflicts of Interest: The authors declare that they have no conflicts of interest to report regarding the present study.

References

Ataizi ZS, Ertilav K, Nazıroğlu M (2019). Mitochondrial oxidative stress-induced brain and hippocampus apoptosis decrease through modulation of caspase activity, Ca^{2+} influx and inflammatory cytokine molecular pathways in the docetaxel-treated mice by melatonin and selenium treatments. *Metabolic Brain Disease* **34**: 1077–1089. DOI 10.1007/s11011-019-00428-x.

Baş E, Nazıroğlu M (2019a). Treatment with melatonin and selenium attenuates docetaxel-induced apoptosis and oxidative injury in kidney and testes of mice. *Andrologia* **51**: e13320.

Baş E, Nazıroğlu M (2019b). Selenium attenuates docetaxel-induced apoptosis and mitochondrial oxidative stress in kidney cells.

Anticancer Drugs **30**: 339–346. DOI 10.1097/CAD.0000000000000723.

Bejarano I, Espino J, Barriga C, Reiter RJ, Pariente JA, Rodríguez AB. (2011). Pro-oxidant effect of melatonin in tumour leucocytes: Relation with its cytotoxic and pro-apoptotic effects. *Basic and Clinical Pharmacology and Toxicology* **108**: 14–20. DOI 10.1111/j.1742-7843.2010.00619.x.

Bossi P, Bergamini C, Miceli R, Bossi P, Bergamini C, Miceli R, Cova A, Orlandi E, Resteghini C, Locati L, Alfieri S, Imbimbo M, Granata R, Mariani L, Iacovelli NA, Huber V, Cavallo A, Licitra L, Rivoltini L (2016). Salivary cytokine levels and oral mucositis in head and neck cancer patients treated with chemotherapy and radiation therapy. *International Journal of Radiation Oncology, Biology, Physics* **96**: 959–966. DOI 10.1016/j.ijrobp.2016.08.047.

Botsoglou NA, Fletouris DJ, Papageorgiou GE, Vassilopoulos VN, Mantis AJ, Trakatellis AG (1994). Rapid, sensitive, and specific thiobarbituric acid method for measuring lipid peroxidation in animal tissue, food, and feedstuff samples. *Journal of Agricultural and Food Chemistry* **42**: 1931–1937. DOI 10.1021/jf00045a019.

Carrasco C, Nazıroğlu M, Rodríguez AB, Pariente JA (2018). Neuropathic pain: Delving into the oxidative origin and the possible implication of transient receptor potential channels. *Frontiers in Physiology* **9**: 95. DOI 10.3389/fphys.2018.00095.

Carrasco C, Rodríguez BA, Pariente JA (2015). Melatonin as a stabilizer of mitochondrial function: Role in diseases and aging. *Turkish Journal of Biology* **39**: 822–831. DOI 10.3906/biy-1504-26.

Chan KK, Glenny AM, Weldon JC (2015). Interventions for the treatment of oral and oropharyngeal cancers: Targeted therapy and immunotherapy. *Cochrane Database of Systematic Reviews* **12**: CD010341.

Childs BG, Baker DJ, Kirkland JL, Campisi J, Deursen JM (2014). Senescence and apoptosis: Dueling or complementary cell fates? *EMBO Reports* **15**: 1139–1153. DOI 10.15252/embr.201439245.

Chrysovergis A, Papanikolaou VS, Tsiambas E, Kikidis D, Maragoudakis P, Ragos V, Kyrodimos E (2019). Caspase complex in laryngeal squamous cell carcinoma. *Journal of the Balkan Union of Oncology* **24**: 1–4.

Donmez Z, Yigit Ö, Bilici S, Dursun N, Gul M, Dastan SD, Uzun H (2016). Evaluation of the antioxidant effects of melatonin on the larynx mucosa of rats exposed to environmental tobacco smoke. *Clinical Otolaryngology* **41**: 211–221. DOI 10.1111/coa.12501.

Ekmekcioglu C (2014). Expression and putative functions of melatonin receptors in malignant cells and tissues. *Wiener Medizinische Wochenschrift* **164**: 472–478. DOI 10.1007/s10354-014-0289-6.

Erel O (2004). A novel automated direct measurement method for total antioxidant capacity using a new generation, more stable ABTS radical cation. *Clinical Biochemistry* **37**: 277–285. DOI 10.1016/j.clinbiochem.2003.11.015.

Gilbert K, Godbout R, Rousseau G (2016). Caspase-3 activity in the rat amygdala measured by spectrofluorometry after myocardial infarction. *Journal of Visualized Experiments* **107**: e53207.

Gökçe SK, Nazıroğlu M (2020). Selenium diminishes docetaxel-induced cell death, oxidative stress, and inflammation in the laryngotracheal epithelium of the mouse. *Biological Trace Element Research* **196**: 184–194. DOI 10.1007/s12011-019-01914-0.

Gomes CJ, Harman MW, Centuori SM, Wolgemuth CW, Martinez JD (2018). Measuring DNA content in live cells by fluorescence microscopy. *Cell Division* **13**: 6. DOI 10.1186/s13008-018-0039-z.

Hara Y, Wakamori M, Ishii M, Maeno E, Nishida M, Yoshida T, Yamada H, Shimizu S, Mori E, Kudoh J, Shimizu N, Kurose H, Okada Y, Imoto K, Mori Y (2002). LTRPC2 Ca^{2+}-permeable channel activated by changes in redox status confers susceptibility to cell death. *Molecular Cell* **9**: 163–173.

Haxel BR, Berg S, Boessert P, Mann WJ, Fruth K (2016). Olfaction in chemotherapy for head and neck malignancies. *Auris Nasus Larynx* **43**: 74–78. DOI 10.1016/j.anl.2015.07.004.

Hoshikawa H, Kamitori K, Indo K, Mori T, Kamata M, Takahashi T, Tokuda M (2018). Combined treatment with D-allose, docetaxel and radiation inhibits the tumor growth in an *in vivo* model of head and neck cancer. *Oncology Letters* **15**: 3422–3428.

Hung CH, Chan SH, Chu PM, Tsai KL (2015). Docetaxel facilitates endothelial dysfunction through oxidative stress via modulation of protein kinase C beta: The protective effects of sotrastaurin. *Toxicological Sciences* **145**: 59–67. DOI 10.1093/toxsci/kfv017.

Ishikawa K, Nakamatsu K, Shiraishi O, Yasuda T, Nishimura Y (2015). Clinical results of definitive-dose (50 Gy/25 fractions) preoperative chemoradiotherapy for unresectable esophageal cancer. *International Journal of Clinical Oncology* **20**: 531–537. DOI 10.1007/s10147-014-0736-9.

Joshi DC, Bakowska JC (2011). Determination of mitochondrial membrane potential and reactive oxygen species in live rat cortical neurons. *Journal of Visualized Experiments* **51**: 2704.

Kahya MC, Nazıroğlu M (2016). Melatonin reduces lens oxidative stress level in STZ-induced diabetic rats through supporting glutathione peroxidase and reduced glutathione values. *Journal of Cellular Neurosciences and Oxidative Stress* **8**: 588–594. DOI 10.37212/jcnos.334113.

Kim J, Lee YJ, Kim YA, Cho ES, Huh E, Bang OS, Kim NS (2017). Aqueous extract of *Phragmitis rhizoma* ameliorates myelotoxicity of docetaxel *in vitro* and *in vivo*. *BMC Complementary and Alternative Medicine* **17**: 393. DOI 10.1186/s12906-017-1890-1.

Kraft R, Grimm C, Frenzel H, Harteneck C (2006). Inhibition of TRPM2 cation channels by N-(p-amylcinnamoyl) anthranilic acid. *British Journal of Pharmacology* **148**: 264–273. DOI 10.1038/sj.bjp.0706739.

Lanza-Jacoby S, Cheng G (2018). 3,3'-Diindolylmethane enhances apoptosis in docetaxel-treated breast cancer cells by generation of reactive oxygen species. *Pharmaceutical Biology* **56**: 407–414. DOI 10.1080/13880209.2018.1495747.

Lawrence RA, Burk RF (1976). Glutathione peroxidase activity in selenium-deficient rat liver. *Biochemical and Biophysical Research Communications* **71**: 952–958. DOI 10.1016/0006-291X(76)90747-6.

Li X, Jiang LH (2018). Multiple molecular mechanisms form a positive feedback loop driving amyloid β42 peptide-induced neurotoxicity via activation of the TRPM2 channel in hippocampal neurons. *Cell Death and Disease* **9**: 195. DOI 10.1038/s41419-018-0270-1.

Mohri J, Katada C, Ueda M, Moriya H, Komori S, Hayakawa K, Koizumi W, Atsuda K (2018). Predisposing factors for chemotherapy-induced nephrotoxicity in patients with advanced esophageal cancer who received combination chemotherapy with docetaxel, cisplatin, and 5-fluorouracil.

Journal of Translational Internal Medicine **6**: 32–37. DOI 10.2478/jtim-2018-0007.

Nazıroğlu M (2009). Role of selenium on calcium signaling and oxidative stress-induced molecular pathways in epilepsy. *Neurochemical Research* **34**: 2181–2191. DOI 10.1007/s11064-009-0015-8.

Nazıroğlu M, Braidy N (2017). Thermo-sensitive TRP channels: Novel targets for treating chemotherapy-induced peripheral pain. *Frontiers in Physiology* **8**: 1040.

Nazıroğlu M, Lückhoff A (2008). A calcium influx pathway regulated separately by oxidative stress and ADP-Ribose in TRPM2 channels: Single channel events. *Neurochemical Research* **33**: 1256–1262. DOI 10.1007/s11064-007-9577-5.

Nemeth C, Humpeler S, Kallay E, Mesteri I, Svoboda M, Rögelsperger O, Klammer N, Thalhammer T, Ekmekcioglu C (2011). Decreased expression of the melatonin receptor 1 in human colorectal adenocarcinomas. *Journal of Biological Regulators & Homeostatic Agents* **25**: 531–542.

Niu L, Deng J, Zhu F, Zhou N, Tian K, Yuan H, Lou H (2014). Anti-inflammatory effect of Marchantin M contributes to sensitization of prostate cancer cells to docetaxel. *Cancer Letters* **348**: 126–134. DOI 10.1016/j.canlet.2014.03.019.

Nopparat C, Chantadul V, Permpoonputtana K, Govitrapong P (2017). The anti-inflammatory effect of melatonin in SH-SY5Y neuroblastoma cells exposed to sublethal dose of hydrogen peroxide. *Mechanisms of Ageing and Development* **164**: 49–60. DOI 10.1016/j.mad.2017.04.001.

Pariente R, Bejarano I, Espino J, Rodríguez AB, Pariente JA (2017). Participation of MT3 melatonin receptors in the synergistic effect of melatonin on cytotoxic and apoptotic actions evoked by chemotherapeutics. *Cancer Chemotherapy and Pharmacology* **80**: 985–998. DOI 10.1007/s00280-017-3441-3.

Reiter RJ, Tan DX, Rosales-Corral SA, Manchester LC (2013). The universal nature, unequal distribution and antioxidant functions of melatonin and its derivatives. *Mini -Reviews in Medicinal Chemistry* **13**: 373–384.

Rodriguez-Garcia A, Mayo JC, Hevia D, Quiros-Gonzalez I, Navarro M, Sainz RM (2013). Phenotypic changes caused by melatonin increased sensitivity of prostate cancer cells to cytokine-induced apoptosis. *Journal of Pineal Research* **54**: 33–45. DOI 10.1111/j.1600-079X.2012.01017.x.

Sakallı Çetin E, Nazıroğlu M, Çiğ B, Övey İS, Aslan Koşar P (2017). Selenium potentiates the anticancer effect of cisplatin against oxidative stress and calcium ion signaling-induced intracellular toxicity in MCF-7 breast cancer cells: Involvement of the TRPV1 channel. *Journal of Receptors and Signal Transduction* **37**: 84–93. DOI 10.3109/10799893.2016.1160931.

Sarıözkan S, Türk G, Eken A, Bayram L, Baldemir A, Doğan G (2017). Gilaburu (*Viburnum opulus* L.) fruit extract alleviates testis and sperm damages induced by taxane-based chemotherapeutics. *Biomedicine and Pharmacotherapy* **95**: 1284–1294. DOI 10.1016/j.biopha.2017.09.057.

Saxena M, Singhal SS, Awasthi YC (1992). A specific, sensitive, and rapid method for the determination of glutathione and its application in ocular tissues. *Experimental Eye Research* **55**: 461–468. DOI 10.1016/0014-4835(92)90119-D.

Shi DD, Dong CM, Ho LC, Lam CTW, Zhou XD, Wu EX, Zhou ZJ, Wang XM, Zhang ZJ (2018). Resveratrol, a natural polyphenol, prevents chemotherapy-induced cognitive impairment: Involvement of cytokine modulation and

neuroprotection. *Neurobiology of Disease* **114**: 164–173. DOI 10.1016/j.nbd.2018.03.006.

Starobova H, Vetter I (2017). Pathophysiology of chemotherapy-induced peripheral neuropathy. *Frontiers in Molecular Neuroscience* **10**: 174. DOI 10.3389/fnmol.2017.00174.

Tabaczar S, Czepas J, Koceva-Chyla A, Kilanczyk E, Piasecka-Zelga J, Gwozdzinski K (2017). The effect of the nitroxide pirolin on oxidative stress induced by doxorubicin and taxanes in the rat brain. *Journal of Physiology and Pharmacology* **68**: 295–308.

Wang H, Li TL, Hsia S, Su IL, Chan YL, Wu CJ (2015). Skeletal muscle atrophy is attenuated in tumor-bearing mice under chemotherapy by treatment with fish oil and selenium. *Oncotarget* **6**: 7758–7773. DOI 10.18632/oncotarget.3483.

Yanar K, Çakatay U, Aydın S, Verim A, Atukeren P, Özkan NE, Karatoprak K, Cebe T, Turan S, Ozkök E, Korkmaz G, Cacına C, Küçükhüseyin O, Yaylım İ. (2016). Relation between endothelial nitric oxide synthase genotypes and oxidative stress markers in larynx cancer. *Oxidative Medicine and Cellular Longevity* **2016**: 4985063.

Zhou Y, Song N, Li X, Han Y, Ren Z, Xu JX, Han YC, Li F, Jia X (2017). Changes in the methylation status of the Oct3/4, Nanog, and Sox2 promoters in stem cells during regeneration of rat tracheal epithelium after injury. *Oncotarget* **8**: 2984–2994. DOI 10.18632/oncotarget.13818.